

Resonant enhancement of the electric field in the grooves of bare metallic gratings exposed to S-polarized light

A. Wirgin

*Laboratoire de Mécanique Théorique, Université Paris VI, 4 Place Jussieu,
F-75230 Paris Cedex 05, France*

A. A. Maradudin

Department of Physics, University of California, Irvine, California 92717

(Received 7 December 1984)

Cavity resonances are shown to be produced for S-polarized light striking an infinitely conducting lamellar grating. They manifest themselves by significant electric field enhancements within the grooves. This result has applications to surface-enhanced Raman scattering.

Much recent research on surface-enhanced effects connected with Raman scattering,¹⁻⁶ second harmonic generation,^{7,8} and photoelectric yield,^{1,9} stresses the role of rough surfaces in general, and gratings in particular, for coupling radiant energy into surface polariton modes responsible for electric field amplification near air-metal (or lossy dielectric) interfaces.¹ Until now, it has been thought^{3,6,8-11} that all resonant near-field enhancement processes at bare gratings are possibly only in the P-polarization state of the excitation radiation (electric vector perpendicular to the rulings, i.e., in the plane of incidence). Hessel and Oliner¹² have predicted, on the basis of an impedance boundary condition, and Andrewartha, Fox, and Wilson¹³ have verified, on the example of a perfectly conducting grating, that gratings are also capable of producing cavity-type resonances with S-polarized light (electric vector parallel to the rulings). These resonances, like their P-polarization counterparts^{11,13} do not occur at the plane-surface plasmon wavelengths. Hessel and Oliner specify that the S resonances will only occur for gratings whose groove depth h satisfies the relation

$$m \lambda_g / 2 > h > (2m - 1) \lambda_g / 4, \quad m = 1, 2, \dots,$$

but they provide us neither with the definition of λ_g nor with the explanation of the origin of this criterion. Andrewartha *et al.* bypass this problem, but they do give us a clear picture of the nature of the resonance poles associated with the cavity modes in the grooves of the grating. In particular, they show that the imaginary part of the (wavelength) resonance pole is generally so large that the S resonance goes unnoticed (i.e., does not appear as an "anomaly" with sharp features as do P resonances) in a far-field observable such as the specular reflectance.

Herein we demonstrate that the S resonances show up in the immediate vicinity of the grating, in particular in the grooves, wherein they give rise to large electric field enhancements when the groove depth h obeys the Hessel and Oliner criterion. The latter is shown to arise from the dispersion relation of a slow guided wave analogous to the S-polarized guided wave that can be supported by a flat lossless dielectric film overlying a flat infinitely conducting substrate.

In a subsequent publication we will show that noble-metal gratings (e.g., Ag) and infinitely conducting gratings of the same profile produce essentially the same kind of S resonances; this enables us to restrict our attention here to the

(simpler) second kind of grating. We treat the same lamellar profile as Andrewartha *et al.*¹³ The plane of incidence (x_1, x_2) cross section of the scattering configuration is displayed in Fig. 1. The rulings are in the \hat{e}_3 direction (with \hat{e}_q the unit vector along the x_q axis). Let $\mathbf{x} = x_1 \hat{e}_1 + x_2 \hat{e}_2$ and let ω be the angular frequency of the incident plane-wave field [the time factor $\exp(-i\omega t)$ is hereafter suppressed]. We designate the incident and total electric fields above the grating by $E_0(\mathbf{x}|\omega)$ and $E_1(\mathbf{x}|\omega)$, respectively, and the component along the x_q axis of $E_p(\mathbf{x}|\omega)$ by $E_{pq}(\mathbf{x}|\omega)$, $p = 0, 1$. The nature and polarization of the incident wave field are such that $E_{pq}(\mathbf{x}|\omega) = 0$, for $p = 0, 1$ and $q = 1, 2$, and $E_{03}(\mathbf{x}|\omega) = \exp(i\mathbf{k}_i \cdot \mathbf{x})$, with $\mathbf{k}_i = \mathbf{k}_{i\parallel} + \mathbf{k}_{i\perp}$, $\mathbf{k}_{i\parallel} = \hat{e}_1(\omega/c)\sin\theta_i$, $\mathbf{k}_{i\perp} = \hat{e}_2(\omega/c)(-\cos\theta_i)$, c being the velocity of light in the medium (assumed to be air) above the grating, and θ_i the angle of incidence.

We adopt the usual Rayleigh plane-wave representation¹² of the field in the half-space above the grooves of the grating:

$$E_{13}(\mathbf{x}|\omega) = E_{03}(\mathbf{x}|\omega) \sum_{n=-\infty}^{\infty} R_n(k_{n\parallel}, \omega) \exp(i\mathbf{k}_n^+ \cdot \mathbf{x}), \quad (1)$$

$$-\infty < x_1 < \infty, \quad x_2 \geq 0+,$$

where

$$\mathbf{k}_n^\pm = \mathbf{k}_{n\parallel}^\pm + \mathbf{k}_{n\perp}^\pm, \quad k_{n\parallel}^\pm = \mathbf{k}_{n\parallel}^\pm \cdot \hat{e}_1, \quad k_{n\perp}^\pm = \mathbf{k}_{n\perp}^\pm \cdot \hat{e}_2,$$

$$\mathbf{k}_{n\parallel}^\pm = \mathbf{k}_{i\parallel} + (2n\pi/d)\hat{e}_1, \quad \lambda = 2\pi c/\omega, \quad (2)$$

$$\mathbf{k}_{n\perp}^\pm = \hat{e}_2[(\omega/c)^2 - (k_{n\parallel}^\pm)^2]^{1/2}, \quad \text{Re}(k_{n\perp}^\pm) + \text{Im}(k_{n\perp}^\pm) \geq 0.$$

Separation of variables enables the following modal

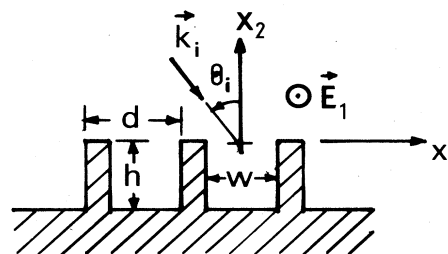


FIG. 1. S-polarization lamellar grating scattering configuration.

representation of the field in the central groove to be obtained:

$$E_{13}(\mathbf{x}|\omega) = \sum_{m=1}^{\infty} A_m(k_{i\parallel}, \omega) \exp(ik_{m\perp}^- h) \sin(\mathbf{k}_{m\parallel}^- \cdot \mathbf{X}) [\exp(i\mathbf{k}_{m\perp}^- \cdot \mathbf{X}) - \exp(-i\mathbf{k}_{m\perp}^- \cdot \mathbf{X})], \quad |x_1| \leq w/2, 0 \leq x_2 \leq h, \quad (3)$$

where

$$\mathbf{X} = \mathbf{x} + (w/2)\hat{\mathbf{e}}_1 + h\hat{\mathbf{e}}_2, \quad \mathbf{k}_{m\parallel}^- = (m\pi/w)\hat{\mathbf{e}}_1. \quad (4)$$

This representation incorporates the boundary condition $E_{13}(\mathbf{x}|\omega) = 0$ on the vertical and bottom horizontal facets of the groove. Applying the boundary condition on the plateaus and the continuity conditions across the central slit results in

$$R_j(k_{i\parallel}, \omega) = -\delta_{j,0} + \gamma \sum_{m=1}^{\infty} A_m(k_{i\parallel}, \omega) [\exp(2ik_{m\perp}^- h) - 1] S_{jm}^-(k_{i\parallel}, \omega), \quad \gamma = w/d, \quad \delta_{l,m \neq l} = 0, \quad \delta_{m,m} = 1; \quad (5)$$

$$A_l(k_{i\parallel}, \omega) = 2[\exp(2ik_{l\perp}^- h) + 1]^{-1} \left[-\left(\frac{k_{l\perp}}{k_{l\perp}^-}\right) S_{0l}^+(k_{i\parallel}, \omega) + \sum_{n=-\infty}^{\infty} R_n(k_{i\parallel}, \omega) \left(\frac{k_{n\perp}^+}{k_{l\perp}^-}\right) S_{nl}^+(k_{i\parallel}, \omega) \right], \quad (6)$$

where

$$S_{jm}^{\pm}(k_{i\parallel}, \omega) = \int_{-w/2}^{w/2} \sin(\mathbf{k}_{m\parallel}^- \cdot \mathbf{X}) \exp(\pm i\mathbf{k}_{j\parallel}^+ \cdot \mathbf{x}) dx_1/w. \quad (7)$$

Equation (5) can be inserted in Eq. (6) to obtain a matrix equation of the type of $\underline{G}\underline{A} = \underline{H}$ for the determination of the vector \underline{A} of the modal amplitudes A_m [the R_j then being computed from the A_m by means of Eq. (5)], or the procedure can be reversed to obtain $\underline{P}\underline{R} = \underline{Q}$ for the determination of the vector \underline{R} of the Rayleigh plane-wave amplitudes R_n [the A_m then being computed from the R_n by means of Eq. (6)]. Hessel and Oliner¹² replace the physical grating by an idealized planar reactance surface whose effect is to approximate \underline{P} by some nearly diagonal matrix \underline{P}' . In the P -polarization state they find that \underline{R} undergoes rapid variations in the neighborhood of a zero of $\det(\underline{P}')$ and that the real part of such a zero (which corresponds to a pole of \underline{R}) occurs near that value of the frequency for which the phase velocity of one of the evanescent waves ($k_{n\perp}^+$ imaginary) in the Rayleigh field becomes equal to that of a surface wave which would be present in some limit-grating configuration (e.g., a flat interface in the case of plane-surface plasmon polaritons).

Andrewartha *et al.*¹³ stick to the rigorous boundary conditions on the physical (lamellar) grating. They solve for \underline{A} (instead of \underline{R}), and associate resonances with the (complex) zeros of $\det(\underline{G})$. The latter are obtained by approximating \underline{G} by \underline{G}' , with $G'_{lm} = 0$ for $l \neq m$ and $G'_{mm} = G_{mm}$. Andrewartha *et al.* indicate that the S resonances do not show up as sharp features in the (far-field) grating efficiencies as do the P resonances, but they do not examine the nature of the near field.

The first step in our approach is to search for solutions to $\underline{G}\underline{A} = \underline{H}$ by truncating it to finite order N and increasing N until what appears as stability of successive solutions is obtained. The solution \underline{A} is then identified with the stabilized value of the solutions. In all the numerical examples herein we obtained stabilization for $N \leq 9$, and found that the $N = 1$ solution furnished a good approximation of the stabilized solution. Results obtained in this manner are displayed in Fig. 2, which shows the real and imaginary parts of $\det(\underline{G})$, for truncation order 9, as a function of the wavelength λ , relative to one of the gratings studied in Ref. 13. Andrewartha *et al.* find the real part of the complex

zeros λ_1^0 and λ_2^0 of $\det(\underline{G}')$ to be located (approximately) at 0.807 and 0.705 μm , respectively. In the figure it will be noticed that $\lambda_m^i < \text{Re}(\lambda_m^0) < \lambda_m^r$, $m = 1, 2$, with λ_m^i and λ_m^r the real zeros of $\text{Im}[\det(\underline{G})]$ and $\text{Re}[\det(\underline{G})]$, respectively (the position of these zeros is essentially the same for $N = 1$). We have found this rule to be verified in the other examples of the paper of Andrewartha *et al.*, but have been unable to establish its theoretical basis. Nevertheless, it furnishes a simple means by which to predict successfully the occurrence of new S resonances.

We have also found λ_m^i and λ_m^r to be identical to the real zeros of $\text{Im}[\det(\underline{P})]$ and $\text{Re}[\det(\underline{P})]$, respectively, the latter being obtained by truncation, as previously. This indicates that the S resonances of Andrewartha *et al.* and those of Hessel and Oliner are probably the same physical objects.

To get a more precise picture of the cavity resonances, we chose a scattering configuration in which the incident wave strikes the grating normally ($\theta_i = 0^\circ$), the grating period is $d = 0.38 \mu\text{m}$, and the wavelength spans the interval $V = [\lambda \in (0.44 \mu\text{m}, 0.76 \mu\text{m})]$ of the visible. This grating

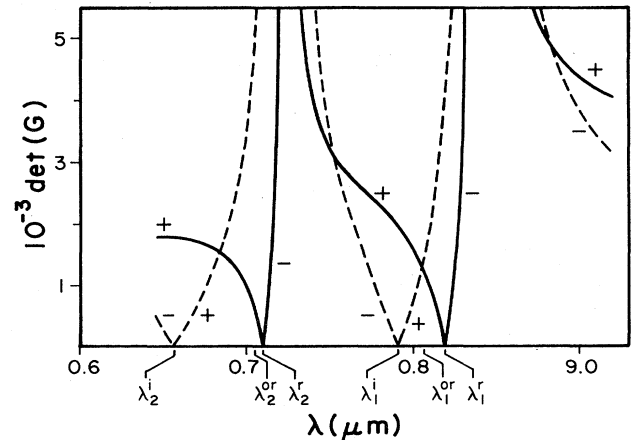


FIG. 2. Real (full curve) and imaginary (dashed curve) parts of $\det(\underline{G})$ vs λ/d . $w/d = 0.43$, $h/d = 1$, $\theta_i = \arcsin(\lambda/2d)$. λ_m^i and λ_m^r designate the locations of the zeros of $\text{Im}[\det(\underline{G})]$ and $\text{Re}[\det(\underline{G})]$, respectively, and the λ_m^{0r} designate the real parts of the complex zeros of $\det(\underline{G}')$ in Ref. 13.

throws all the incident energy into the specular ($n=0$) spectral order throughout V so that it is impossible to find any trace of S resonances in a far-field intensity. How then is one to detect the resonances? The aforementioned examination of the positions of the zeros of the real and imaginary parts of $\det(\underline{G})$ suggests a means for establishing the conditions of existence of the resonances which is particularly efficient if the groove field is monomode ($k_{m\perp}$ imaginary for $m > 1$). This is assured over V if $w=0.35 \mu\text{m}$. We then find that the question of the location of the zeros of $\text{Re}[\det(\underline{G})]$ and $\text{Im}[\det(\underline{G})]$ reduces, to a good approximation, to that of the location of the zeros $\tilde{\lambda}_m^i$ and $\tilde{\lambda}_m^r$ of

$$D'(0, \omega) = k_{\perp\perp} + 4\gamma |k_{\perp\perp}^+| S_{\perp\perp}^-(0, \omega) S_{\perp\perp}^+(0, \omega) \tan(k_{\perp\perp} h), \quad (8)$$

$$D^i(0, \omega) = 2\gamma k_{0\perp}^+ S_{0\perp}^-(0, \omega) S_{0\perp}^+(0, \omega) \tan(k_{\perp\perp} h). \quad (9)$$

From the latter relation, we find that the $\tilde{\lambda}_m^i$ are the roots of $\tan(k_{\perp\perp} h) = 0$, i.e.,

$$\tilde{\lambda}_m^i = 2[(m/h)^2 + 1/w]^2)^{-1/2}; \quad m = 1, 2, \dots \quad (10)$$

The roots $\tilde{\lambda}_m^r$ turn out to be larger than $\tilde{\lambda}_m^i$ for each m , with the distance of $\tilde{\lambda}_m^r$ to $\tilde{\lambda}_m^i$ being smaller the smaller m is. By comparison with the results of Andrewartha *et al.*, we found that this distance is a measure of the imaginary part of the complex zero λ_m^0 , and thus of the damping of the resonance associated with λ_m^0 . We have also found that the real part of the resonance pole of \underline{A} is located in the interval $[\tilde{\lambda}_m^i, \tilde{\lambda}_m^r]$ very close to the root $\tilde{\lambda}_m^i$ of

$$\hat{D}(0, \omega) = k_{\perp\perp} + \gamma |k_{\perp\perp}^+| \tan(k_{\perp\perp} h) = 0. \quad (11)$$

This is analogous to the dispersion relation for an S -polarized slow guided surface wave on a flat lossless dielectric film overlying a flat, infinitely conducting substrate. The condition of existence of a cavity resonance is therefore similar to that of a guided-surface wave polariton,¹⁴ viz., $\tan(k_{\perp\perp} h) < 0$. This is identical to the Hessel and Oliner criterion if λ_g is identified with $2\pi/k_{\perp\perp}$. Our numerical experiments on the aforementioned scattering configuration show that the excitation of the guided wave is accompanied by the (weaker) excitation of a host of other evanescent waves in the Rayleigh field. The interference of these waves produces a field in the half-space above the grooves of the grating whose magnitude is essentially the same as that of the field above a perfect mirror. This means that the resonances not only fail to manifest themselves in the

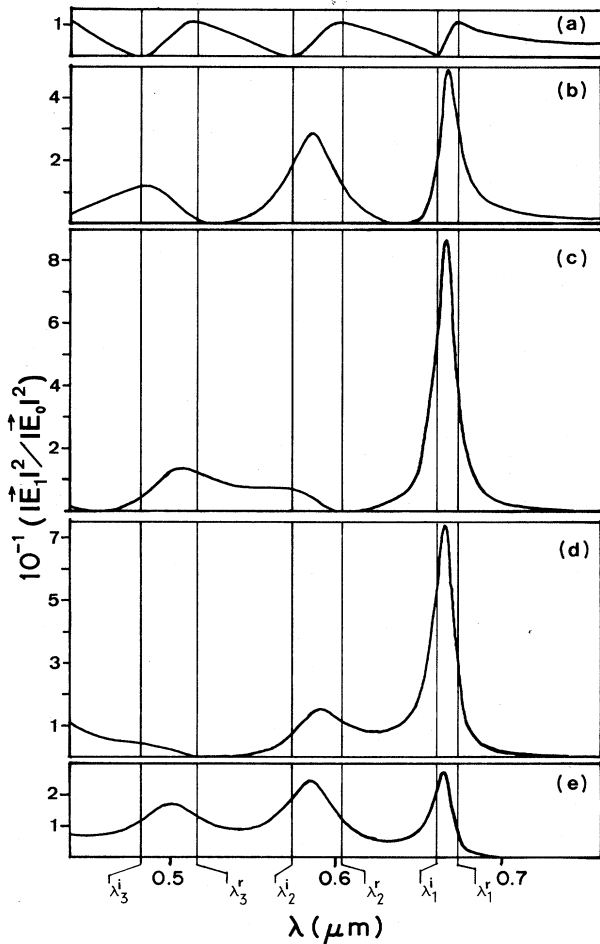


FIG. 3. Electric field enhancement on the line $x_1=0$ of the central groove vs λ . $d=0.38 \mu\text{m}$, $w=0.35 \mu\text{m}$, $h=1 \mu\text{m}$, $\theta_i=0^\circ$. Samples (a), (b), (c), (d), and (e) are taken at $x_2=0, -0.2h, -0.4h, -0.6h$, and $-0.8h$, respectively. The vertical lines indicate the positions of the roots λ_m^i and λ_m^r . The cavity resonances occur in the intervals $[\lambda_m^i, \lambda_m^r]$, $m=1, 2, \dots$

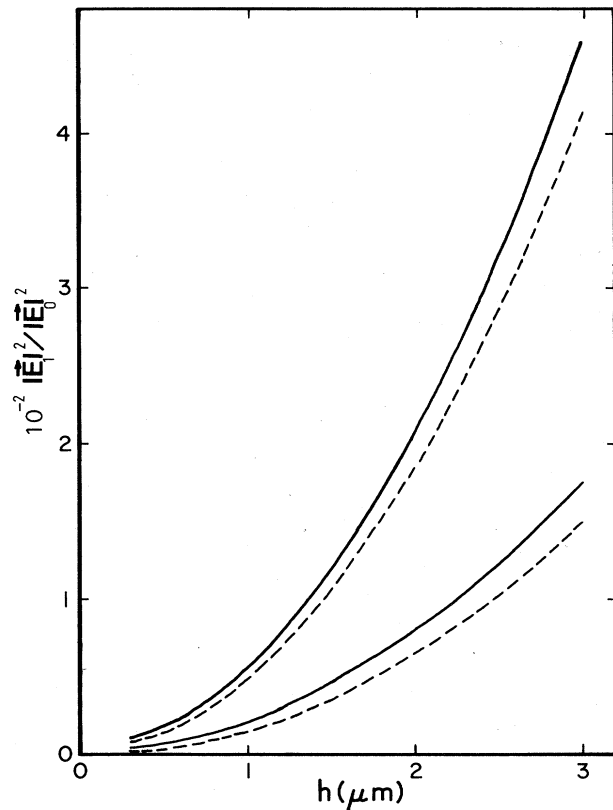


FIG. 4. Electric field enhancement in the central groove as a function of groove depth h . $d=0.38 \mu\text{m}$, $w=0.35 \mu\text{m}$, $\theta_i=0^\circ$, $\lambda=\tilde{\lambda}_1^i$, with $\tilde{\lambda}_1^i$ defined by Eq. (10). Solid lines apply to a perfect conductor, dashed lines to silver. Upper pair of curves applies to location $x_1=0, x_2=-0.4h$; lower pair to $x_1=0, x_2=-0.8h$.

far-field intensities, but also in the intensity of the near field above the groove cavities.

The situation is radically different within the grooves, although it is quite similar at $\tilde{\lambda}_m^i$, $\tilde{\lambda}_m$, and $\tilde{\lambda}_m^r$, especially for $m=1$. At $\tilde{\lambda}_m^i$ and $x_2 = -fh$ ($0 < f \leq 1$)

$$|E_{13}(0, x_2 | \omega)| = 4 |k_{1\perp} S_{01}^\dagger(0, \omega)| \left| \frac{\sin[k_{1\perp}(x_2 + h)]}{k_{1\perp}} \right|, \quad (12)$$

which is larger the smaller is $k_{1\perp}$ at $\tilde{\lambda}_m^i$. The optimal condition occurs for $m=1$ and $\tilde{\lambda}_m^i$ as close as possible to $2w$. The latter situation is obtained for $h \rightarrow \infty$. These facts are made evident in Fig. 3, in which are displayed the (modulus squared) electric field enhancements as functions of λ , and in Fig. 4, in which they are plotted versus h at the wavelength $\tilde{\lambda}_m^i$ defined in Eq. (10) which, for $m=1$, is very close to the wavelength at which the enhancements are greatest. In this respect, our Fig. 4 is similar to Fig. 6(b) in Ref. 4 wherein it is found that the field enhancement asso-

ciated with the excitation of the plane plasmon of an Ag grating at first increases with increasing h , and then past some critical value $h = h_c$ begins to decrease with further increase in h due to radiation damping. We find the enhancement at resonance (identified with $\tilde{\lambda}_1^i$) to increase monotonically with h ; this is maintained for a highly conducting metal such as Ag and is consistent with the finding of Andrewartha *et al.* according to which the imaginary part of the complex zeros associated with the cavity resonances tends to zero as $h \rightarrow \infty$. Thus, both the positions and damping effects of the cavity resonances are very different from those of the plane-plasmon polariton resonances.

These results suggest that a possible way of observing the S resonances is to measure the degree of enhancement of Raman scattered light from molecules adsorbed within the grooves of a grating.

This work was supported in part by National Science Foundation Grant No. DMR-82-14214.

- ¹H. Metiu, in *Surface Enhanced Raman Scattering*, edited by R. K. Chang and T. E. Furtak (Plenum, New York, 1982), p. 1.
²A. Girlando, M. R. Philpott, D. Heitman, J. D. Swalen, and R. Santo, *J. Chem. Phys.* **72**, 5187 (1980).
³S. S. Jha, J. R. Kirtley, and J. C. Tsang, *Phys. Rev. B* **22**, 3973 (1980).
⁴M. Weber and D. L. Mills, *Phys. Rev. B* **27**, 2698 (1983).
⁵N. García, *Opt. Commun.* **45**, 307 (1983).
⁶N. E. Glass, A. A. Maradudin, and V. Celli, *J. Opt. Soc. Am.* **73**, 1240 (1983).
⁷C. K. Chen, A. R. B. de Castro, and Y. R. Shen, *Phys. Rev. Lett.*

- 46**, 145 (1981).
⁸R. Reinisch and M. Nevière, *Phys. Rev. B* **24**, 4392 (1981).
⁹J. G. Endriz and W. E. Spicer, *Phys. Rev. B* **4**, 4159 (1971).
¹⁰N. García and A. A. Maradudin, *Opt. Commun.* **45**, 301 (1983).
¹¹T. Lopez-Rios and A. Wirgin, *Solid State Commun.* **52**, 197 (1984).
¹²A. Hessel and A. A. Oliner, *Appl. Opt.* **4**, 1275 (1965).
¹³J. R. Andrewartha, J. R. Fox, and I. J. Wilson, *Opt. Acta* **26**, 69 (1979).
¹⁴K. L. Kliewer and R. Fuchs, *Phys. Rev.* **144**, 495 (1966).